Hippocampal plasticity requires postsynaptic ephrinBs

Ilona C Grunwald[1,7], Martin Korte[2,7], Giselind Adelmann[3], Anne Plueck[4], Klas Kullander[5], Ralf H Adams[6], Michael Frotscher[3], Tobias Bonhoeffer[2,7] & Rüdiger Klein[1,7]

Chemical synapses contain specialized pre- and postsynaptic structures that regulate synaptic transmission and plasticity. EphB receptor tyrosine kinases are important molecular components in this process. Previously, EphB receptors were shown to act postsynaptically, whereas their transmembrane ligands, the ephrinBs, were presumed to act presynaptically. Here we show that in mouse hippocampal CA1 neurons, the Eph/ephrin system is used in an inverted manner: ephrinBs are predominantly localized postsynaptically and are required for synaptic plasticity. We further demonstrate that EphA4, a candidate receptor, is also critically involved in long-term plasticity independent of its cytoplasmic domain, suggesting that ephrinBs are the active signaling partner. This work raises the intriguing possibility that depending on the type of synapse, Eph/ephrins can be involved in activity-dependent plasticity in converse ways, with ephrinBs on the pre- or the postsynaptic side.

Long-lasting changes in synaptic function are thought to be the cellular basis for learning and memory and for activity-dependent plasticity during development. Most of the work on synaptic plasticity has concentrated on excitatory synapses that use glutamate as their neurotransmitter. Glutamate is released by the presynaptic neuron and binds to postsynaptic AMPA or NMDA receptors. Whereas AMPA receptors open in response to glutamate alone and mediate most of the rapid excitatory postsynaptic current (EPSC), NMDA receptors open only if the postsynaptic membrane is depolarized. Differential activation of NMDA receptors can either lead to long-term potentiation (LTP) or long-term depression (LTD) of a synapse. These two opposing forms of synaptic plasticity are thought to help fine-tune neural connections and may serve to store information in the brain.

The EphB2 receptor[1–3], a member of the B subclass of Eph receptor tyrosine kinases[4,5], is thought to act postsynaptically by modulating glutamate receptors[1–3]. In young cultured neurons, EphB2 directly interacts with NMDA receptors[6,7] and thereby modulates Ca^{2+} influx into the postsynaptic cells. At the mossy fiber synapse, postsynaptic EphB2 receptors interact with the PDZ-domain protein GRIP (glutamate receptor interacting protein) to mediate AMPA receptor–dependent LTP[3]. The subcellular localization of the ligands of EphB2 receptors, so-called B-type ephrins, has not been investigated directly. Because of their reverse signaling potential[8], it has been suggested that they are located presynaptically as part of a trans-synaptic signaling cascade[3].

Our present results support a new role for transmembrane ephrinBs. We show that ephrinBs are predominantly localized at the postsynaptic side of CA3-CA1 synapses. We further show that conditional genetic ablation of ephrinB2 or ephrinB3 causes strong defects in LTP and LTD in hippocampal slices. Lack of EphA4, a high-affinity receptor for ephrinB2 and ephrinB3, results in a comparable defect in LTP, suggesting a functional interaction at the synapse. Interestingly, EphA4 forward-signaling is not required, as the deficit is rescued by an EphA4 receptor with the intracellular domain completely deleted. This suggests that EphA4 does not act as a receptor in the traditional sense, but rather as a ligand for postsynaptic and possibly presynaptic ephrinBs competent for reverse signaling. Our data, together with other reports[1,3], support a model in which the Eph/ephrin signaling system is used for activity-dependent plasticity in a converse fashion at different hippocampal synapses.

RESULTS

EphrinBs are localized postsynaptically at CA3-CA1 synapses

In a previous study[2], we used *in situ* hybridization to map the spatial distribution of mRNAs encoding ephrinB2 and ephrinB3 in specific subpopulations of hippocampal neurons. The hippocampus contains three main excitatory synapses: the perforant path connects the entorhinal cortex to dentate gyrus (DG) neurons, the mossy fibers connect DG neurons to neurons in the CA3 region, and the Schaffer collaterals connect CA3 neurons to CA1 neurons (**Fig. 1a**). With respect to the CA3-CA1 pathway, both ephrinB2 and ephrinB3 mRNAs are highly enriched in CA1 neurons, as judged by *in situ* hybridization analysis[2]. Using densitometric analysis of *in situ* hybridization signals, we estimated approximately ten times more ephrinB2 mRNA in postsynaptic CA1 relative to CA3 neurons (pixels

---

[1]Department of Molecular Neurobiology and [2]Department of Cellular and Systems Neurobiology, Max-Planck Institute of Neurobiology, 82152 Munich-Martinsried, Germany. [3]Institute for Anatomy and Cell Biology, University of Freiburg, 79001 Freiburg, Germany. [4]Institute for Genetics, University of Cologne, 50931 Köln, Germany. [5]Department of Medical Biochemistry, Gothenburg University, 40530 Gothenburg, Sweden. [6]Cancer Research UK - London Research Institute, London WC2A 3PX, UK. [7]These authors contributed equally to this work. Correspondence should be addressed to T.B. (tobias.bonhoeffer@neuro.mpg.de) or R.K. (rklein@neuro.mpg.de).

Figure 1 Postsynaptic expression of ephrinBs. (**a**) Nissl stained section of a wild-type adult hippocampus. Neurons from the dentate gyrus form synapses onto CA3 neurons (mossy fibers), CA3 neurons connect to CA1 neurons (Schaffer collaterals). (**b**) *ephrinB2* mRNA is abundant in CA1 and hardly detectable in CA3. Quantification using NIH image software. Ten equally sized areas (examples shown as little squares) were selected in CA1 and CA3 and their intensities were compared. A randomly chosen region was subtracted as background (bg). (**c**) EphrinB proteins are enriched in the postsynaptic density (PSD). Different PSD subfractions, non-PSD fractions and total forebrain homogenates were compared by western blot analysis for their content of ephrinBs and Eph receptors. EphrinBs localize to the triton-insoluble fractions of the PSD, whereas two of their cognate receptors, EphA4 and EphB2, were abundant in non-PSD fractions. Postsynaptic proteins PSD95, GRIP1 and GluR2 were enriched in PSD fractions, whereas presynaptic synaptophysin was excluded from the PSD. (**d**–**g**) CA1-region synapses immunolabeled with ephrinB2 antibody and analyzed by EM. (**d**–**f**) EphrinB2 protein was found at about 40% of all CA1 region synapses. Labeling was predominant at or close to the postsynaptic density of synapses (38% postsynaptic [black arrowhead] versus 12% presynaptic [white arrowhead] of all synapses). (**g**) Labeling was strongly reduced in ephrinB2-deficient synapses. The asterisk indicates the presynaptic side of each synapse shown. (**h**) Summary data for all synapses analysed in *ephrinB2*[lx/lx] and *ephrinB2-CamKcre* mice (*n* = 2 mice per group). Note that postsynaptic labeling was more affected than presynaptic labeling in *ephrinB2-CamKcre* compared to *ephrinB2*[lx/lx] controls.
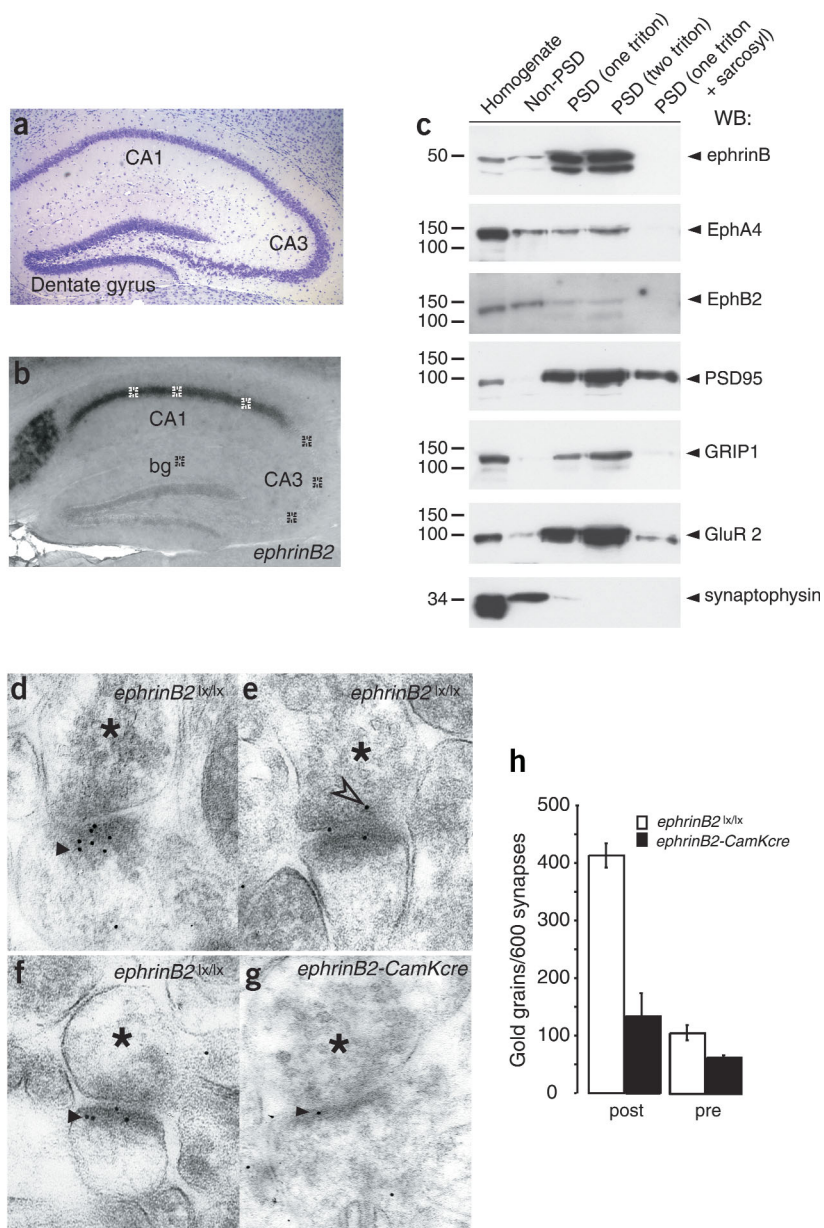

in CA3 were 11.7 ± 2.9% of those in CA1, *n* = 3; **Fig. 1b,h**). This raises the possibility that ephrinBs participate in the regulation of synaptic transmission in postsynaptic neurons, possibly as part of the postsynaptic density (PSD). To obtain evidence that ephrinBs localize to the PSD, we prepared PSD fractions from adult forebrain using standardized sucrose gradient fractionations and triton/sarcosyl extraction[9]. Our PSD preparations were highly enriched in characteristic PSD proteins such as PSD95, GRIP1 and the AMPA-type glutamate receptor subunit GluR2 (refs. 10–13), whereas the presynaptic marker synaptophysin was absent in all PSD fractions (**Fig. 1c**). In western blot analysis using anti-ephrinB antibodies, we found ephrinBs strongly enriched in the postsynaptic density and barely detectable in non-PSD fractions; EphB2 and EphA4 were found in all fractions (**Fig. 1c**). These data do not contradict previous ultrastructural findings[14] on postsynaptic localization of EphB2 and EphA4, they rather provide evidence that EphB2 and EphA4 are also present at other neuronal sites, possibly at presynaptic terminals. To directly visualize ephrinB2 at the CA3-CA1 synapse, we applied immunoelectron microscopic analysis using a specific ephrinB2 antibody. We found about four times (4.0 ± 0.28, *n* = 2) more ephrinB2 labeling at the postsynaptic side of CA1 synapses than at presynaptic terminals of the same region (**Fig. 1d–f,h**). We obtained proof for specificity of

ephrinB2 staining by comparing staining in wild-type and ephrinB2-deficient hippocampi (*ephrinB2-CamKcre*, **Fig. 1g,h**). These data show that with respect to CA3-CA1 synapses, ephrinBs are more abundant at the postsynaptic side.

Normal morphology of ephrinB mutant hippocampus

Given the unexpected postsynaptic localization of ephrinBs at CA1-CA3 synapses, we sought to investigate their role in synaptic plasticity. Because germline-removal of ephrinB2 leads to early embryonic lethality due to failure in vascular remodeling[15,16], we generated a conditional allele of ephrinB2 (*ephrinB2*[lx]; **Fig. 2a,b**) and used a CamKIIα promoter–driven Cre recombinase[17] to specifically remove ephrinB2 from the postnatal forebrain. In homozygous *ephrinB2*[lx/lx] mutants carrying one copy of the *CamKIIα-cre* transgene (*ephrinB2-CamKcre* mice), ephrinB2 mRNA was removed from the adult hippocampus and ephrinB2 protein levels were strongly reduced in hippocampus and cortex, but not cerebellum (**Fig. 2c,d**).

Figure 2 Forebrain-specific removal of ephrinB2. (**a**) Schematic representation of the ephrinB2 conditional targeting vector. The *lox*P sites for recombination by Cre recombinase were introduced around exon 2. The *neo* gene cassette was flanked by FRT (Flp recombinase target) sites for removal by crossing to Flp deleter mice[38]. (**b**) Homologous recombination verified by Southern hybridization with ES cell genomic DNA following enzymatic restriction by *Hind*III (H). Probe 1 (indicated in **a**) was used to detect wild-type (3.5 kb) and mutant (5.6 kb) DNA fragments in two independent ES cell clones. Probe 2 shows that the mutant band is positive for the *neo* resistance gene. (**c**,**d**) *EphrinB2*$^{lx/lx}$ mice (after removal of the *neo* gene) were crossed to *CamKIIα-cre* transgenic animals[17] to specifically remove ephrinB2 from the forebrain. (**c**) *In situ* hybridization analysis for ephrinB2 and ephrinB3 mRNAs in control *ephrinB2*$^{lx/lx}$ and mutant *ephrinB2-CamKcre* mice. Note that the expression of ephrinB2 is greatly reduced, whereas ephrinB3 mRNA is unchanged in mutant mice. (**d**) Immunoprecipitation/western blot analysis of P70 hippocampus (hi), neocortex (co) and cerebellum (ce) from the indicated mice using a specific ephrinB2 antibody showing that ephrinB2 protein is downregulated in cortex and hippocampus, but not cerebellum. Western blot analysis using antibody to tubulin shows that equal amounts of protein were compared.
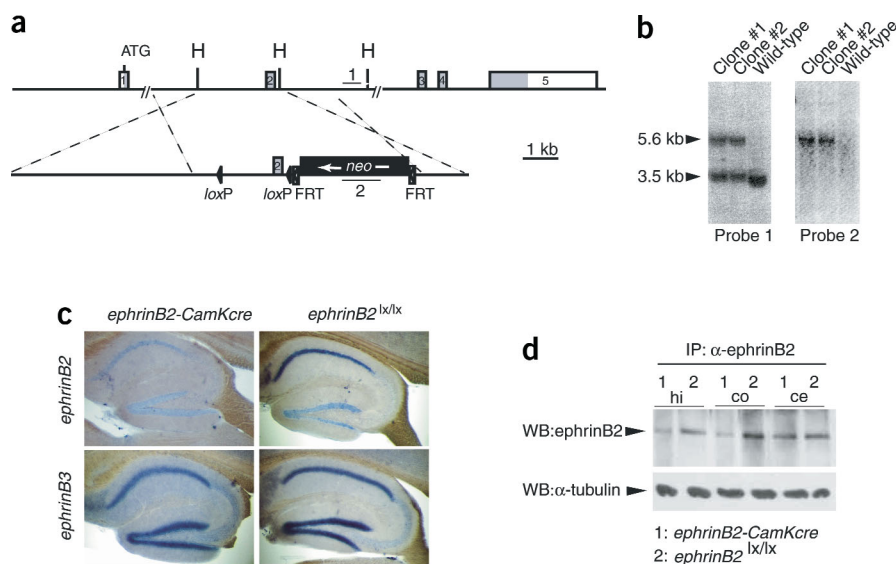
EphrinB2-CamKcre mice did not show any gross alterations of the neuronal architecture of the hippocampus nor obvious behavioral abnormalities (data not shown).

Recent reports suggest that ephrinBs, EphB2 and EphA4 receptors are involved in the formation of synapses and spines[6,18–20]. We therefore performed electron microscopic analysis of all mutant lines used in this study and their respective littermate controls to determine whether synapse morphology was altered in any of them. We found no structural difference in CA1 synapses in any of the mutant mice analyzed. Equally, width of synaptic cleft, appearance of the PSD and number of presynaptic vesicles appeared similar in all samples (**Fig. 3a–d** and **Supplementary Fig. 1** online).

Focusing on the role of ephrinB2 and its candidate receptor EphA4, we quantified the number of CA1 region synapses in *ephrinB2-CamKcre*, *ephA4*$^{-/-}$ (ephA4 null), and *ephA4*$^{EGFP/EGFP}$ mice (a signaling deficient knock-in of EphA4, see below) and found no significant difference in synapse number
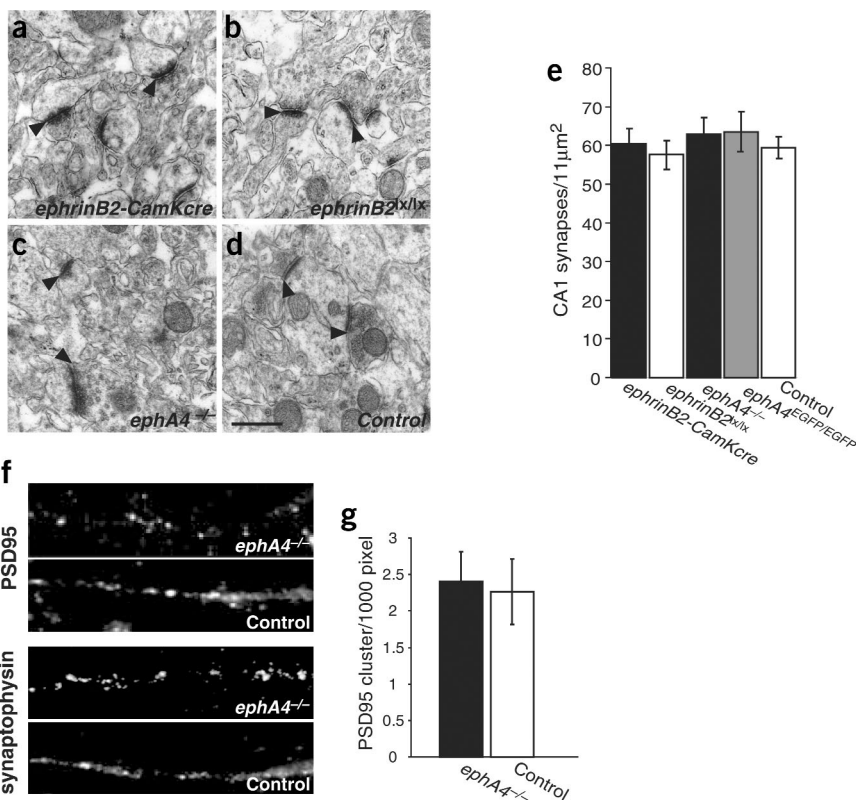

Figure 3 Ultrastructure of synapses in mutant mice. (**a**–**d**) Electron micrographs showing morphology of synapses in the CA1 region of adult brains derived from the indicated mutants and littermate controls. PSDs are indicated by arrowheads. Scale bar (**d**), 0.7 μm. Additional micrographs are provided in **Supplementary Fig. 1**. (**e**) Quantification of synapses in the CA1 region of *ephrinB2-CamKcre*, *ephrinB2*$^{lx/lx}$, *ephA4*$^{-/-}$, *ephA4*$^{EGFP/EGFP}$ and controls ($n = 3$ mice, >500 synapses per animal counted). The graph shows the average number of synapses in a 11 μm^2 CA1 region. No significant difference in number of synapses was found between different groups. (**f**) Hippocampal neurons from embryos at 7 d.i.v. from *ephA4*$^{-/-}$ mice and littermate controls were immunostained using anti-PSD95 and anti-synaptophysin antibodies. No obvious changes in pre- (synaptophysin) or postsynaptic (PSD95) specializations were observed in *ephA4*$^{-/-}$ neurons compared to control cultures ($n = 2$ embryos, 45 neurons in each group). (**g**) Quantification of postsynaptic specializations (PSD95 positive clusters/1,000 pixels of neurite) in *ephA4*$^{-/-}$ neurons compared to littermate controls ($P = 0.51$, *t*-test).

Figure 4 EphrinBs are critical for LTP. (**a**) Left, paired pulse facilitation (PPF) of the fEPSP at various interstimulus intervals (ISI) from *ephrinB2-CamKcre* slices (*n* = 15 slices) and control *ephrinB2*[lx/lx] slices (*n* = 15 slices, *P* > 0.05, *t*-test). Error bars = s.e.m. Right, fEPSP at various stimulus intensities (FV, fiber volley). In the range of 0.2–0.8 mV both groups showed similar values (*ephrinB2-CamKcre*, *n* = 13 slices, *ephrinB2*[lx/lx], *n* = 13 slices, *P* > 0.05, *t*-test). Only at 1 mV intensity, *ephrinB2-CamKcre* slices showed a significant increase in fEPSP compared to controls (*P* = 0.04, *t*-test). (**b**) LTP was induced by stimulation of presynaptic CA3 neurons with TBS. *EphrinB2-CamKcre* mice show a strong deficit in early CA3-CA1 LTP compared to littermate controls (124.8% in mutants versus 169.8% in controls at 55–60 min after TBS, *P* < 0.001, *t*-test). LTP levels in control animals stayed significantly higher than in *ephrinB2-CamKcre* mice even at late phase LTP (118.6% in mutants versus 154.1% in controls at 175–180 min after TBS, JJNL (*P* < 0.01, *t*-test). (**c**) *EphrinB3* null mutant slices show normal PPF (left, *ephrinB3*^{−/−}, *n* = 7 slices; control, *n* = 6 slices, *P* > 0.05, *t*-test) and no significant changes in fEPSP (right, *ephrinB3*^{−/−}, *n* = 9 slices; control, *n* = 8 slices, *P* > 0.05, *t*-test). (**d**) *ephrinB3*^{−/−} slices display a strong defect in CA3-CA1 LTP (118.7% in mutants versus 145.7% in controls at 55–60 min after TBS, *P* < 0.01).
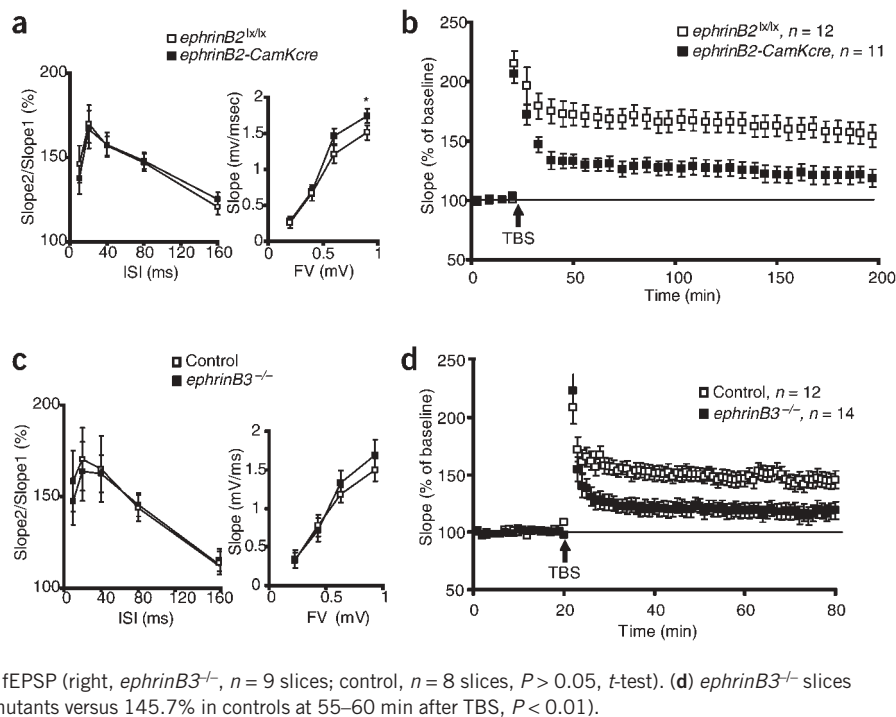
compared to littermate controls (*n* = 3 mice per genotype, >500 synapses counted per animal, **Fig. 3e**). These findings are in agreement with a recent study showing that only the removal of multiple EphB receptors (EphB1, EphB2, EphB3) leads to significant changes in spine morphology and number in the hippocampus[21]. We further addressed whether removal of EphA4 would influence the number of pre- and postsynaptic specializations *in vitro*. We cultured hippocampal neurons from *ephA4*^{−/−} and control littermates for 7 days *in vitro* (d.i.v.) and analyzed synaptic specializations using immunofluorescence analysis (**Fig. 3f**). We found no significant difference in number of postsynaptic PSD95-immunoreactive puncta compared to controls (*P* > 0.05, **Fig. 3f,g**). No obvious difference between mutants and controls was seen comparing staining of the presynaptic marker synaptophysin (**Fig. 3f**). Since EphB2 receptors directly interact with NR1 subunits of the NMDA receptor, we used immuno electron microscopy to quantify the number of NR1 subunits at ephrinB2-deficient synapses compared to controls. We found no significant difference in the number of NR1-labeled synapses in mutants compared to controls (33 ± 2.9% in *ephrinB2-CamKcre* (*n* = 2) compared to 34 ± 0.8% in *ephrinB2*[lx/lx] (*n* = 2), *P* = 0.8, *t*-test). Furthermore, labeled synapses contained similar numbers of gold particles in both groups (1.52 ± 0.06 in *ephrinB2-CamKcre* (*n* = 2) compared to 1.56 ± 0.03 in *ephrinB2*[lx/lx] (*n* = 2), *P* = 0.6, *t*-test).

EphrinB2 and ephrinB3 are required for CA3-CA1 LTP

Before investigating long-term changes in synaptic plasticity, we analyzed wild-type and mutant mice with respect to basal synaptic transmission. Extracellular recordings of the CA3-CA1 pathway in *ephrinB2-CamKcre* mice did not reveal significant deficiencies in basal parameters of synaptic transmission such as paired-pulse facilitation (PPF), post tetanic potentiation (PTP) after thetaburst stimulation (TBS), and the size of the presynaptic fiber volley (PSFV) (*P* > 0.05, **Fig. 4a**). Also, the amplitude of field excitatory postsynaptic potentials (fEPSPs) was similar in the mutants (**Fig. 4a**) except at the strongest presynaptic stimulation (1 mV), which is considerably higher than the

one used in subsequent experiments (approx. 0.2 mV). Because of the ephrinB-regulated interaction of EphB2 receptors with the NMDA receptor[6], we also analyzed the NMDA-component of the EPSP signal. In the presence of the AMPA receptor antagonist DNQX, *ephrinB2-CamKcre* slices showed an EPSP signal which was indistinguishable from littermate *ephrinB2*[lx/lx] control slices. The signal was completely NMDA-dependent and disappeared in the presence of the NMDA receptor antagonist AP-5 (**Supplementary Fig. 2** online).

To investigate a requirement for ephrinB2 in CA3-CA1 hippocampal LTP, we used TBS in acute hippocampal slices, a stimulus known to efficiently induce long-lasting LTP[22] (see Methods). After recording a stable baseline, a TBS stimulus was given to fibers of the CA3 presynaptic neurons and LTP was recorded from CA1 neurons for up to 3 hours post stimulation. Comparison of *ephrinB2-CamKcre* with littermate *ephrinB2*[lx/lx] controls revealed a strong reduction in LTP (118.6 ± 6.5% in mutants versus 154.1 ± 8.7% in controls at 175–180 min after TBS application, *t*-test, *P* < 0.001, **Fig. 4b** and **Supplementary Fig. 3** online). These data demonstrate that ephrinB2 is critical for hippocampal LTP.

We next investigated the role of ephrinB3, which shows the highest expression of all ephrinBs in the mouse hippocampus[2] (**Fig. 2c**). We used previously generated germline-targeted knockouts of *ephrinB3*, which are viable and fertile, however, display midline guidance defects in the spinal cord[23,24]. Like *ephrinB2-CamKcre* mice, *ephrinB3* mutants do not show any obvious morphological defects in the hippocampus (data not shown and **Supplementary Fig. 1** online), nor do they display significant defects in basal synaptic transmission parameters and NMDA receptor–dependent EPSP (*P* > 0.05, **Fig. 4c** and **Supplementary Fig. 2** online). Using the same TBS stimulation protocol, we found that ephrinB3 is required at least for early stages of LTP, closely resembling the ephrinB2 phenotype (118.7 ± 7.2% in mutants versus 145.7 ± 8.5% in controls at 55–60 min after TBS, *t*-test, *P* < 0.01; **Fig. 4d**). Taken together, these data implicate both ephrinB2 and ephrinB3 in NMDA receptor–dependent forms of hippocampal long-term potentiation.
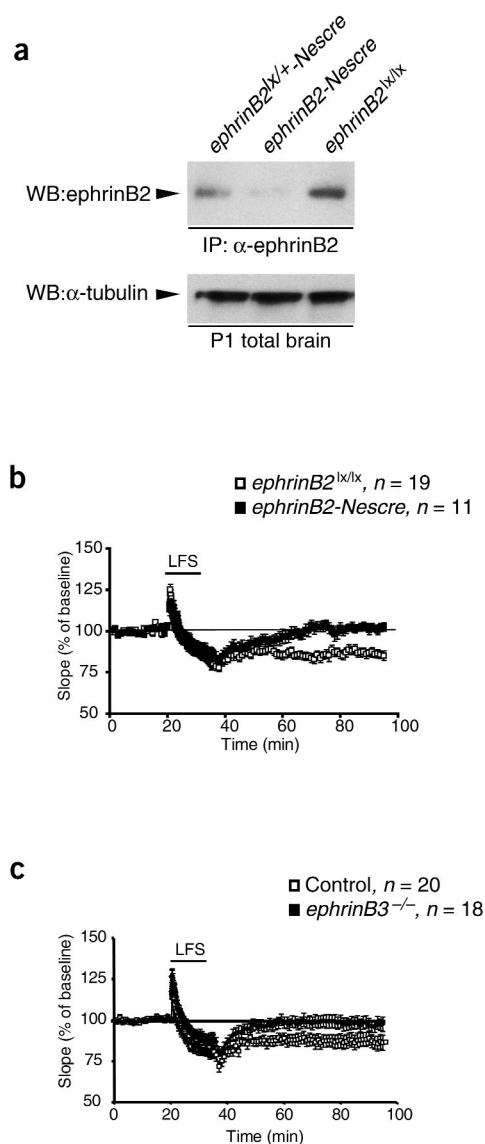
a

WB:ephrinB2 ►

IP: α-ephrinB2

WB:α-tubulin ►

P1 total brain

b

□ *ephrinB2*$^{lx/lx}$, *n* = 19
■ *ephrinB2-Nescre*, *n* = 11

c

□ Control, *n* = 20
■ *ephrinB3*$^{−/−}$, *n* = 18

Figure 5 EphrinBs are required for LTD. (**a**) Immunoprecipitation/western blot analysis of ephrinB2 protein from P1 brains of the indicated mice. EphrinB2 levels were reduced by ~90% in *ephrinB2-Nescre* conditional knockouts, and by ~50% in heterozygotes compared to *ephrinB2*$^{lx/lx}$ control brains. (**b**) ephrinB2 is required for LTD in young hippocampal slices (P15–P20). LFS induced a significant long-lasting decrease of fEPSP in control slices but not in *ephrinB2-Nescre* slices (101.1% in mutants versus 86.6% in controls at 55–60 min after LFS, *P* < 0.01, *t*-test). (**c**) *ephrinB3* knockout slices show a strong LTD defect. Note that the EPSP quickly returned to baseline in mutant compared to wild-type control slices (97.1% in mutants versus 86.1% in controls at 55–60 min after LFS, *P* < 0.05, *t*-test).

EphrinB2 and ephrinB3 are required for long-term depression
Since our earlier experiments on animals lacking EphB2 receptor revealed a deficit not only in hippocampal LTP but also in long-term depression (LTD) we analyzed hippocampal LTD in the CA3-CA1 pathway of ephrinB mutants. *CamKIIα-cre*-mediated recombination does not start until postnatal day 15 (P15)[17], but LTD is most prominent at early postnatal stages (P15–20)[25,26]. We therefore used the *Nestin-Cre* transgenic line[27] to remove ephrinB2 from the developing nervous system (*ephrinB2-Nescre* mice). Immunoprecipitation and subsequent western blot analysis on brain samples taken from P1 mice showed a dose-dependent reduction of ephrinB2 protein levels compared to controls (**Fig. 5a**). As found with *ephrinB2-CamKcre* mice, early loss of ephrinB2 did not alter the fundamental circuitry nor ultrastructure of the hippocampus (data not shown and **Supplementary Fig. 1** online). After recording baseline responses of acute hippocampal slices for 20 min, a low frequency stimulation (LFS) of 900 stimuli at 1 Hz was given (15 min). *ephrinB2-Nescre* slices significantly diverged from *ephrinB2*$^{lx/lx}$ control slices (**Fig. 5b**). While *ephrinB2*$^{lx/lx}$ control slices showed a persistent decrease in fEPSPs, which lasted for at least 100 min, the *ephrinB2-Nescre* slices

returned to baseline at 70 min (101.6 ± 2.4% in mutants versus 86.6 ± 2.6% in controls at 55–60 min after LFS, *t*-test, *P* < 0.01; **Fig. 5b**). *EphrinB3* knockout animals showed a very similar defect in LTD (97.1 ± 3.9% in mutants versus 86.1 ± 4.3% in controls at 55–60 min after LFS, *t*-test, *P* < 0.05; **Fig. 5c**) only that the effect is visible earlier. These findings indicate a strong requirement for both ephrinB2 and ephrinB3 in LTD.

EphA4 is a candidate receptor for postsynaptic ephrinBs
Our earlier work had indicated a requirement for EphB2 in late phases of CA3-CA1 LTP[2]. Present findings indicate that ephrinBs were required already at early stages. We therefore addressed the potential role of another Eph receptor that interacts with ephrinB2 and ephrinB3 during early phase LTP. The one Eph receptor for which there is ample evidence for *in vivo* interaction with ephrinB2 and ephrinB3 is EphA4. EphA4 interaction with ephrinB2 or ephrinB3 regulates cell migration at segment boundaries[28] and axon guidance at the midline[24,29]. EphA4 is expressed throughout all regions of the adult hippocampus[2], but lack of it does not disrupt hippocampal architecture (data not shown). As observed for ephrinB mutants, *ephA4*$^{−/−}$ mutants show normal basal synaptic transmission parameters and NMDA receptor component (**Fig. 6a** and **Supplementary Fig. 2** online). To test if LTP was affected, we again analyzed the CA3-CA1 pathway of wild-type controls and *ephA4*$^{−/−}$ mice. In contrast to *ephB2*$^{−/−}$ (ref. 2) and *ephB3*$^{−/−}$ mice (unpublished data) and similar to *ephrinB2* and *ephrinB3* mutants, *ephA4*$^{−/−}$ slices showed a marked decrease in early phase LTP (120.4 ± 7.3% in mutants versus 144.7 ± 6.7% in controls at 55–60 min after TBS; *t*-test, *P* < 0.01; **Fig. 6b**). This similar time course of LTP defects, together with the fact that EphA4 is a high affinity receptor for ephrinB2 and ephrinB3, suggests that EphA4 may serve as a critical interaction partner for ephrinB2 and ephrinB3 in the formation of early phase CA3-CA1 LTP.

Signaling-deficient EphA4 rescues plasticity defects
Because of the bi-directional signaling capabilities of the Eph/ephrinB system, we next investigated the requirements for EphA4 cytoplasmic domains and forward signaling in this system. We specifically asked, if EphA4 acts as a signaling receptor or, alternatively, as an activating agent for signaling competent postsynaptic ephrinBs. To disrupt all signaling potential of EphA4 (as opposed to kinase signaling only), we generated a novel knock-in allele encoding a truncated form of EphA4, in which the entire cytoplasmic domain and thus all potential intracellular binding sites, was replaced with enhanced green-fluorescent protein (EGFP) (**Fig. 6c,d**). Homozygous *ephA4*$^{EGFP/EGFP}$ mice were viable and moderately fertile. Western blot analysis on hippocampal lysates of heterozygous *ephA4*$^{EGFP/+}$ mice revealed a smaller EphA4-EGFP isoform, which was expressed at similar levels to wild-type EphA4 protein (**Fig. 6e**). Homozygous

Figure 6 Signaling-independent requirement of EphA4 in LTP and LTD. (**a**) Left, PPF at various ISIs from *ephA4⁻/⁻* slices (*n* = 9) and control slices (*n* = 8, *P* > 0.05, *t*-test) and fEPSPs at various intensities (*ephA4⁻/⁻*, *n* = 10; control, *n* = 7; *P* > 0.05, *t*-test) compared to controls. (**b**) LTP in the CA3-CA1 pathway induced by TBS. *EphA4⁻/⁻* slices show a strong defect (114.3% in mutants versus 139.5% in controls at 175–180 min after TBS, *P* < 0.01, *t*-test). (**c**) Left, schematic representation of the *ephA4-EGFP* allele encoding a forward-signaling deficient isoform of EphA4. The entire cytoplasmic tail was replaced by the coding sequence of enhanced GFP. Right, gene-targeting strategy used to generate *ephA4-EGFP* knock-in mice. A cDNA encoding EphA4-EGFP was inserted in frame into exon 3 by homologous recombination. (**d**) Homologous recombination verified by Southern hybridization with ES cell genomic DNA following enzymatic restriction by *Bam*HI (B). The 3′ probe (indicated in panel **c**) was used to detect wild-type (12 kb) and mutant (5 kb) DNA fragments in selected ES cell clones. (**e**) Using a monoclonal antibody against the extracellular part of EphA4, expression levels of wild-type EphA4 and EphA4-EGFP in adult brains derived from the indicated mice are shown. Heterozygotes show similar levels of both isoforms. Stripping and subsequent reprobing of the western blot with an antibody against EGFP identified the lower band as EphA4-EGFP. (**f**) LTP in the CA3-CA1 pathway is rescued in *ephA4-EGFP* knock-in slices. No differences were found in early or late LTP in *ephA4*EGFP/EGFP knock-in slices when compared to their wild-type controls (146.4% in mutants versus 146.9% in controls at 175–180 min after TBS, *P* = 0.27). (**g,h**) LTD induced by LFS. (**g**) *EphA4⁻/⁻* slices show a strong defect compared to controls (85.0% in controls versus 100.4% in mutants, *P* < 0.01, *t*-test). (**h**) *ephA4*EGFP/EGFP knock-in slices rescue EphA4-dependent LTD (94.9% in mutants versus 92.2% in controls at 55–60 min after LFS, *P* = 0.8, *t*-test).
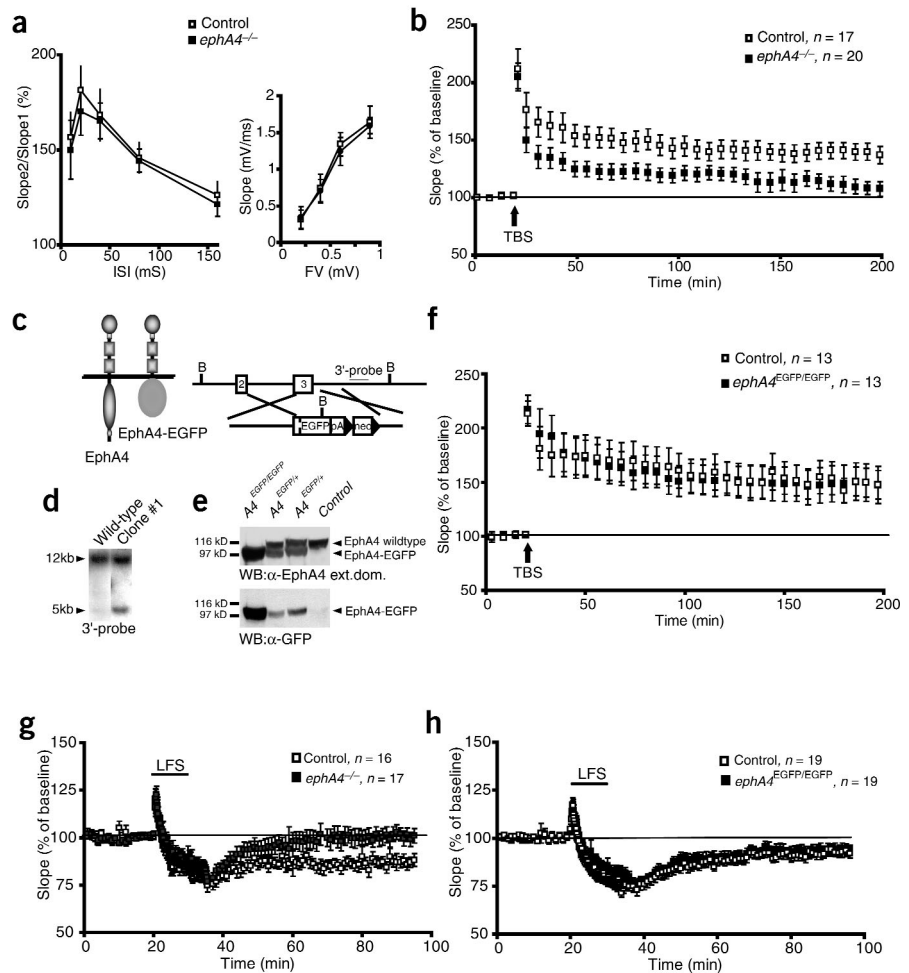
*ephA4*EGFP/EGFP mice, instead, only expressed the smaller EphA4-EGFP isoform. Behaviorally, the *ephA4*EGFP/EGFP mice show the same rabbit-like hopping gait as the *ephA4* null and *ephA4* kinase-dead mutants[29–31], indicating that this allele indeed disrupts the kinase-dependent functions of EphA4 at the spinal cord midline.

To test whether signaling-deficient EphA4-EGFP was able to rescue synaptic plasticity we tested LTP induced by TBS in wild-type and *ephA4*EGFP/EGFP mice and found it to be completely normal (146.4 ± 17.3% in mutants versus 146.9 ± 12.9% in littermate controls 175–180 min after TBS, *t*-test, *P* > 0.1; **Fig. 6f**). A similar rescue was observed in the case of LTD: following the LFS, control slices exhibited strong LTD while slices lacking EphA4 showed considerably reduced LTD (85.0 ± 2.8% in controls versus 100.4 ± 3.2% in mutants at 55–60 min after LFS, *t*-test, *P* < 0.001; **Fig. 6g**). In contrast, we found no significant differences in the rate of LTD induction nor in the amount of LTD between *ephA4*EGFP/EGFP slices and slices derived from wild-type littermates (94.9 ± 3.1% in mutants versus 92.2 ± 2.9% in controls at 55–60 min after LFS, *P* = 0.8, *t*-test; **Fig. 6h**) indicating that the cytoplasmic domain of EphA4 is not required for long-term plasticity at CA3-CA1 synapses. Considering the postsynaptic localization of ephrinB2 at CA3-CA1 synapses, our findings suggest that EphA4 acts as a non-signaling partner for postsynaptic ephrinBs.

DISCUSSION

Our study provides evidence for a novel postsynaptic role for ephrinBs in NMDA receptor–dependent forms of long-term plasticity. Previous models pictured ephrinBs as ligands on the presynaptic terminal activating postsynaptic EphB2 receptors, which interact with NMDA receptors or AMPA receptors[3,6,7,32,33]. The results presented here together with previous work[3] suggest instead that the bi-directional ephrin/Eph signaling system is used differently depending on the synapses involved. At the mossy fiber–CA3 synapse, ephrinB3 is specifically expressed by presynaptic dentate gyrus cells while the EphB2 receptor is expressed by both, presynaptic dentate gyrus and postsynaptic CA3 neurons. At this synapse, EphB2 receptors specifically interact with postsynaptic proteins to regulate LTP[3]. Our work on the synapse between CA3 and CA1 neurons shows that ephrinBs, in this case, are localized mainly postsynaptically in CA1 neurons, while the relevant Eph receptors are expressed both by pre- and postsynaptic neurons. Importantly, both EphB2 and EphA4 receptors show a signaling-independent requirement in long-term plasticity suggesting reverse signaling by postsynaptic ephrinBs. We cannot exclude that the presynaptic fraction of ephrinB2, although significantly smaller and less reduced in the *ephrinB2-CamKcre* mutants, has a component in the plasticity defects that we detect.

Why would evolution select for such 'receptor-ligand' reciprocity, which to our knowledge has no precedent? One possibility could be that the alternating expression patterns of ephrinBs reflect some developmental, yet functionally redundant role, similar to their role in the hindbrain, where ephrins help to compartmentalize cells into segments. Because ephrinBs are capable of reverse signaling, they may have acquired a postsynaptic signaling function in neuronal plasticity in addition to their developmental role. This would be analogous to their cell-autonomous signaling function in specific growth cone guidance situations. For example, commissural axon guidance seems to require ephrinB reverse signaling in a cell-autonomous manner, whereas the relevant Ephs act in neighboring cells not requiring kinase signaling[29,34]. Alternatively, morphogenesis of the hippocampus happens independently of the ephrin/Eph system and the ephrinB expression pattern is only a reflection of clear molecular and functional differences between different populations of hippocampal neurons and their synapses. Different populations of neurons have developed distinct requirements for long-term plasticity (e.g., changes in NMDA receptor signaling), and postsynaptic ephrinBs are part of the machinery that mediates postsynaptic modifications during NMDA receptor–dependent LTP[2,22,33]. It is possible that postsynaptic ephrinBs function at other central synapses outside the hippocampus. Other bi-directional signaling systems, such as transmembrane semaphorins, were recently shown to function either pre- or postsynaptically during synaptogenesis[35] and may display similar reciprocity during synaptic plasticity.

EphA4 has recently been shown to modulate spine formation in hippocampal slices in vitro and to regulate aspects of spine formation in vivo[19]. These effects were mediated by EphA4 forward signaling. Our work instead shows a signaling-independent role for EphA4 in CA3-CA1 long-term plasticity, suggesting parallel functions and distinct mechanisms during plasticity and spine formation. Similarly, the observed interaction of EphB2 with NMDA receptor and the EphB2-mediated enhancement of NMDA receptor channel function may be primarily important during development for synaptogenesis, rather than for adult plasticity. Consistent with this scenario, we did not find a change in basic functions of NMDA receptor activity nor in the number in NR1 subunits in CA3-CA1 synapses in ephrinB2 mutants. Moreover, the present study implicates EphA4 as a relevant interaction partner for ephrinB ligands in synaptic plasticity, and EphA4 receptors are not capable of directly interacting with NMDA receptors[6].

A number of issues remain unanswered. For instance, which aspect of postsynaptic signaling is modulated by ephrinBs, and do ephrinBs or Ephs also signal in presynaptic cells? What role does internalization of the Eph/ephrinB complex, a process that was recently shown to regulate the cellular response to Eph/ephrin signaling[36,37], have at the synapse? And, is Eph receptor action kinase-independent for the first stages of LTP/LTD, whereas subsequent processes like the generation of spines require kinase signaling[19]? These questions are beyond the scope of the present work but we are beginning to address some of them by conditionally removing Ephs from presynaptic CA3 or postsynaptic CA1 neurons.

We have identified a requirement for ephrinB reverse signaling in postsynaptic CA1 neurons. This raises the intriguing possibility that the bi-directional Eph/ephrin signaling system is used for activity-dependent plasticity in converse ways at different synapses.

METHODS

Mice. The generation and genotypic analysis of ephA4^{−/−} and ephrinB3^{−/−} mutant mice and transgenic cre lines have been previously described[23,29]. For the generation of ephrinB2 conditional mice, a 2.2-kb genomic region containing the second exon of the murine ephrinB2 gene was flanked by loxP sites. The targeting construct also contained adjacent 8.5 kb (5′) and 1.2 kb (3′) genomic DNA fragments for homologous recombination as well as a neomycin (neo) resistance cassette (**Fig. 2b**). The presence of the 5′ loxP site in transfected E14.1 embryonic stem (ES) cells was confirmed by PCR. We removed the neo cassette by cross-breeding with transgenic mice expressing Flp recombinase[38], and all experimental analysis was done with conditional ephrinB2[lx/lx] mice negative for both Flp and neo. EphA4[EGFP] mice were generated using the same targeting strategy as described previously[29]. Briefly, a cDNA containing the extracellular region of EphA4 fused to EGFP was inserted in frame into exon III. Successful recombination was analyzed by PCR strategy and Southern blot analysis (**Fig. 6c,d**). All mutant mice were maintained in a heterozygous state on a 129xC57Bl/6 background. For all experiments, the F1 generation from a heterozygous cross was used. Animal experiments were performed under a permit from the State Government of Bavaria.

Primary cell culture and immunofluorescence. Cortical and hippocampal neuron cultures were prepared from E16.5 CD1 mouse embryos as described previously[2]. Detection of specific antigens in cultured primary neurons was done as described previously[2]. Labeling was quantified using MetaMorph imaging analysis. All images were collected using the same parameters at a Zeiss axiophot. Images were scaled and stained clusters were automatically counted using MetaMorph software.

Postsynaptic density fractionation. PSD fractions were prepared essentially as described[9] using forebrains of six adult mice per preparation.

Electron microscopy. Ultrastructural analysis of CA1 region synapses was accomplished as described previously[2].

EM immunocytochemistry. EphrinB2-CamKcre and control ephrinB2[lx/lx] mice were anesthetized with Narkodorm-n (250 mg per kg body weight) and transcardially perfused with 0.9% saline followed by a fixative containing 4% paraformaldehyde, 0.1% glutaraldehyde and 0.2% picric acid in 0.1 M phosphate buffer (pH 7.4). Brains were removed and post-fixed in the same fixative overnight, cut on a vibratome into 300-μm sections, and the CA1 area of the hippocampus was excised. Tissue blocks were cryoprotected in glycerol, cryofixed in nitrogen-cooled propane, substituted in methanol containing 1.5% uranylacetate and embedded in Lowicryl HM20 (Chemische Werke Lowi). Ultrathin sections were processed for post-embedding immunocytochemistry, using a polyclonal antibody against the NR1 subunit of the NMDA receptor (5 μg protein/ml; Chemicon) and a polyclonal antibody against ephrinB2 (2 μg protein/ml; R&D Systems). Immunolabeling was visualized by 10 nm gold-coupled secondary antibodies (1:20, British BioCell International). Direct comparisons between synapses of ephrinB2-CamKcre and ephrinB2[lx/lx] mice were made on sections processed simultaneously. On each grid, 300 randomly selected synapses were counted in CA1 stratum radiatum, and the number of labeled PSDs among these contacts as well as the number of gold grains per individual PSD were evaluated.

In situ hybridization analysis. In situ hybridization experiments were done as previously described[2].

Slice electrophysiology. LTD experiments were performed with mice 14–20 d old (P14–P20), and mice used for LTP experiments were P40–P80. For each experimental condition, acute slices of 4–6 animals were used. Synaptic responses were evoked in the CA3 region of the hippocampus by stimulating Schaffer collaterals with 0.1-ms pulses. Field excitatory postsynaptic potentials (fEPSPs) were recorded extracellularly in the stratum radiatum of CA1 region using glass microelectrodes (Clark) filled with 3M NaCl (5–20 MΩ). For baseline recordings, slices were stimulated at 0.1 Hz for 20 min at stimulation intensities of 40–100 μA. To induce LTD, a 1-Hz stimulus train was delivered for 15 min (900 stimuli) at baseline stimulus intensity. LTP was induced by applying theta-burst stimulation (TBS) consisting of three bursts (10-s interval), each composed of ten trains (5 Hz) with four pulses (100 Hz) each. Paired-pulse facilitation (PPF) was tested by applying two pulses separated by inter-stimulus-intervals (ISI) ranging from 10–160 ms. PPF was expressed as the increase

ARTICLES

in initial slope of the second fEPSP relative to the first. Electrophysiological data were sampled at 5 kHz on a PC using LabView (National Instruments). As an indicator of synaptic strength the initial slope of the evoked fEPSPs was calculated. All measurements were carried out and analyzed in a strictly blind fashion. To analyze the functionality of the NMDA receptor fEPSPs were recorded in the following sequence: after 15-min baseline recording 10 μM DNQX (6,7-dinitroquinoxaline 2,3-dione; Sigma) in low Mg^{2+} (0.5mM) ACSF was bath-applied. After 15 min 50 μM AP-5 (DL-2-amino-5-phosphonovalerate; Sigma) together with DNQX was added for 20 min to the same slice in low Mg^{2+} ACSF; afterwards normal ACSF was used for washout.

Note: Supplementary information is available on the Nature Neuroscience website.

1. Henderson, J.T. *et al.* The receptor tyrosine kinase EphB2 regulates NMDA-dependent synaptic function. *Neuron* **32**, 1041–1056 (2001).
2. Grunwald, I.C. *et al.* Kinase-independent requirement of EphB2 receptors in hippocampal synaptic plasticity. *Neuron* **32**, 1027–1040 (2001).
3. Contractor, A. *et al.* Trans-synaptic Eph receptor-ephrin signaling in hippocampal mossy fiber LTP. *Science* **296**, 1864–1869 (2002).
4. Wilkinson, D.G. Multiple roles of EPH receptors and ephrins in neural development. *Nat. Rev. Neurosci.* **2**, 155–164 (2001).
5. Palmer, A. & Klein, R. Multiple roles of ephrins in morphogenesis, neuronal networking, and brain function. *Genes Dev.* **17**, 1429–1450 (2003).
6. Dalva, M.B. *et al.* EphB receptors interact with NMDA receptors and regulate excitatory synapse formation. *Cell* **103**, 945–956 (2000).
7. Takasu, M.A., Dalva, M.B., Zigmond, R.E. & Greenberg, M.E. Modulation of NMDA receptor-dependent calcium influx and gene expression through EphB receptors. *Science* **295**, 491–495 (2002).
8. Kullander, K. & Klein, R. Mechanisms and functions of Eph and ephrin signalling. *Nat. Rev. Mol. Cell. Biol.* **3**, 475–486 (2002).
9. Cho, K.O., Hunt, C.A. & Kennedy, M.B. The rat brain postsynaptic density fraction contains a homolog of the *Drosophila* discs-large tumor suppressor protein. *Neuron* **9**, 929–942 (1992).
10. Walikonis, R.S. *et al.* Identification of proteins in the postsynaptic density fraction by mass spectrometry. *J. Neurosci.* **20**, 4069–4080 (2000).
11. Chen, L. *et al.* Stargazin regulates synaptic targeting of AMPA receptors by two distinct mechanisms. *Nature* **408**, 936–943 (2000).
12. Dong, H., Zhang, P., Liao, D. & Huganir, R.L. Characterization, expression, and distribution of GRIP protein. *Ann. NY Acad. Sci.* **868**, 535–540 (1999).
13. Wyszynski, M. *et al.* Association of AMPA receptors with a subset of glutamate receptor-interacting protein *in vivo*. *J. Neurosci.* **19**, 6528–6537 (1999).
14. Buchert, M. *et al.* The junction-associated protein AF-6 interacts and clusters with specific Eph receptor tyrosine kinases at specialized sites of cell-cell contact in the brain. *J. Cell Biol.* **144**, 361–371 (1999).
15. Wang, H.U., Chen, Z.F. & Anderson, D.J. Molecular distinction and angiogenic interaction between embryonic arteries and veins revealed by ephrin-B2 and its receptor Eph-B4. *Cell* **93**, 741–753 (1998).
16. Adams, R.H. *et al.* Roles of ephrinB ligands and EphB receptors in cardiovascular development: demarcation of arterial/venous domains, vascular morphogenesis, and sprouting angiogenesis. *Genes Dev.* **13**, 295–306 (1999).
17. Minichiello, L. *et al.* Essential role for TrkB receptors in hippocampus-mediated learning. *Neuron* **24**, 401–414 (1999).
18. Ethell, I.M. *et al.* EphB/syndecan-2 signaling in dendritic spine morphogenesis. *Neuron* **31**, 1001–1013 (2001).
19. Murai, K.K., Nguyen, L.N., Irie, F., Yamaguchi, Y. & Pasquale, E.B. Control of hippocampal dendritic spine morphology through ephrin-A3/EphA4 signaling. *Nat. Neurosci.* **6**, 153–160 (2003).
20. Penzes, P. *et al.* Rapid induction of dendritic spine morphogenesis by trans-synaptic ephrinB-EphB receptor activation of the Rho-GEF kalirin. *Neuron* **37**, 263–274 (2003).
21. Henkemeyer, M., Itkis, O.S., Ngo, M., Hickmott, P.W. & Ethell, E.M. Multiple EphB receptor tyrosine kinases shape dendritic spines in the hippocampus. *J. Cell Biol.* (in press).
22. Bliss, T.V. & Collingridge, G.L. A synaptic model of memory: long-term potentiation in the hippocampus. *Nature* **361**, 31–39 (1993).
23. Kullander, K. *et al.* Ephrin-B3 is the midline barrier that prevents corticospinal tract axons from recrossing, allowing for unilateral motor control. *Genes Dev.* **15**, 877–888 (2001).
24. Yokoyama, N. *et al.* Forward signaling mediated by ephrin-B3 prevents contralateral corticospinal axons from recrossing the spinal cord midline. *Neuron* **29**, 85–97 (2001).
25. Dudek, S.M. & Bear, M.F. Homosynaptic long-term depression in area CA1 of hippocampus and effects of N-methyl-D-aspartate receptor blockade. *Proc. Natl. Acad. Sci. USA* **89**, 4363–4367 (1992).
26. Mulkey, R.M. & Malenka, R.C. Mechanisms underlying induction of homosynaptic long-term depression in area CA1 of the hippocampus. *Neuron* **9**, 967–975 (1992).
27. Tronche, F. *et al.* Disruption of the glucocorticoid receptor gene in the nervous system results in reduced anxiety. *Nat. Genet.* **23**, 99–103 (1999).
28. Mellitzer, G., Xu, Q. & Wilkinson, D.G. Eph receptors and ephrins restrict cell intermingling and communication. *Nature* **400**, 77–81 (1999).
29. Kullander, K. *et al.* Kinase-dependent and kinase-independent functions of EphA4 receptors in major axon tract formation *in vivo*. *Neuron* **29**, 73–84 (2001).
30. Dottori, M. *et al.* EphA4 (Sek1) receptor tyrosine kinase is required for the development of the corticospinal tract. *Proc. Natl. Acad. Sci. USA* **95**, 13248–13253 (1998).
31. Kullander, K. *et al.* Role of EphA4 and EphrinB3 in local neuronal circuits that control walking. *Science* **299**, 1889–1892 (2003).
32. Ghosh, A. Neurobiology. Learning more about NMDA receptor regulation. *Science* **295**, 449–451 (2002).
33. Murai, K.K. & Pasquale, E.B. Can Eph receptors stimulate the mind? *Neuron* **33**, 159–162 (2002).
34. Henkemeyer, M. *et al.* Nuk controls pathfinding of commissural axons in the mammalian central nervous system. *Cell* **86**, 35–46 (1996).
35. Godenschwege, T.A., Hu, H., Shan-Crofts, X., Goodman, C.S. & Murphey, R.K. Bi-directional signaling by Semaphorin 1a during central synapse formation in *Drosophila*. *Nat. Neurosci.* **5**, 1294–1301 (2002).
36. Zimmer, M., Palmer, A., Kohler, J. & Klein, R. EphB-ephrinB bi-directional endocytosis terminates adhesion allowing contact mediated repulsion. *Nat. Cell Biol.* **5**, 869–878 (2003).
37. Marston, D.J., Dickinson, S. & Nobes, C.D. Rac-dependent trans-endocytosis of ephrinBs regulates Eph-ephrin contact repulsion. *Nat. Cell Biol.* **5**, 879–888 (2003).
38. Dymecki, S.M. A modular set of Flp, FRT and lacZ fusion vectors for manipulating genes by site-specific recombination. *Gene* **171**, 197–201 (1996).